Available online at www.sciencedirect.com
SCIENCE DIRECT®
Il Farmaco 58 (2003) 659–668
IL FARMACO
www.elsevier.com/locate/farmac

3D QSAR studies for the β-tubulin binding site of microtubule-stabilizing anticancer agents (MSAAs) A pseudoreceptor model for taxanes based on the experimental structure of tubulin

Laura Maccari, Fabrizio Manetti, Federico Corelli, Maurizio Botta *

Dipartimento Farmaco Chimico Tecnologico, Università degli Studi di Siena, Via Aldo Moro, I-53100 Siena, Italy

Received 25 November 2002; accepted 20 January 2003

Abstract

The antimitotic agent paclitaxel continues to play an important role in the cancer chemotherapy. However, its inefficacy on certain resistant cells and toxic side effects have led to the search of new taxanes with improved biological activity. By means of a pseudoreceptor modeling approach, we have developed a binding site model for a series of taxanes. It is the first 3D QSAR model derived from the experimentally determined tubulin structure obtained by electron crystallography studies. The model is able to correlate quantitatively the structural properties of the studied compounds with their biological data.

Keywords: Pseudoreceptor modeling; 3D QSAR; Tubulin; Taxanes

1. Introduction

Paclitaxel (Taxol®) is the most prominent microtubule inhibitor currently used in cancer chemotherapy.

Paclitaxel is a member of the taxane diterpenoids containing the unusual β-phenylisoserine side-chain esterifying the C-13 position and the singular oxetane ring (compound **1**, Scheme 1, Tables 1 and 2). It has been approved by the Food and Drug Administration (FDA) for the treatment of drug-resistant ovarian cancer, in 1992, and for the treatment of breast cancer, in 1994. At present, paclitaxel is the best-selling anticancer drug in history, used for the treatment of breast and ovarian cancers, squamous cancers of the head and neck, as well as for non-small cell lung cancer, small-cell lung cancer, and other types of cancers [1].

Docetaxel (Taxotere®, compound **9**, Scheme 1, Tables 1 and 2), a semisynthetic analogue of **1** with a similar activity, is also currently in clinical practice [2].

The mechanism of action of **1** has been extensively investigated [3–5]. It was the first compound found to promote the polymerization of tubulin into microtubules and to stabilize pre-formed microtubules [6,7]. In particular, the interaction between paclitaxel and β-tubulin alters the normal microtubule dynamics leading finally to cell apoptosis [8,9].

The tubulin–microtubule system represents the target for other anticancer drugs acting with the same mechanism of action of **1** (epothilones [10], discodermolide [11], eleutherobins [12,13], sarcodictyins [13], and laulimalide [14]) or acting as microtubule depolymerizing agents (colchicine [15], vinblastine [16], and vincristine [17]). Although chemists are also enormously interested in new antimitotic agents, due to the evident success of paclitaxel, new taxoids have been investigated in order to overcome its disadvantages (i.e., low aqueous solubility, multi-drug resistance) and improve its biological activity. As a consequence of such huge amount of work, at least three novel taxanes are currently undergoing Phase I/II clinical development [18].

Based on our efforts to find theoretical quantitative models describing the relationships between structure

* Corresponding author.
E-mail address: botta@unisi.it (M. Botta).

0014-827X/03/$ - see front matter
doi:10.1016/S0014-827X(03)00099-5

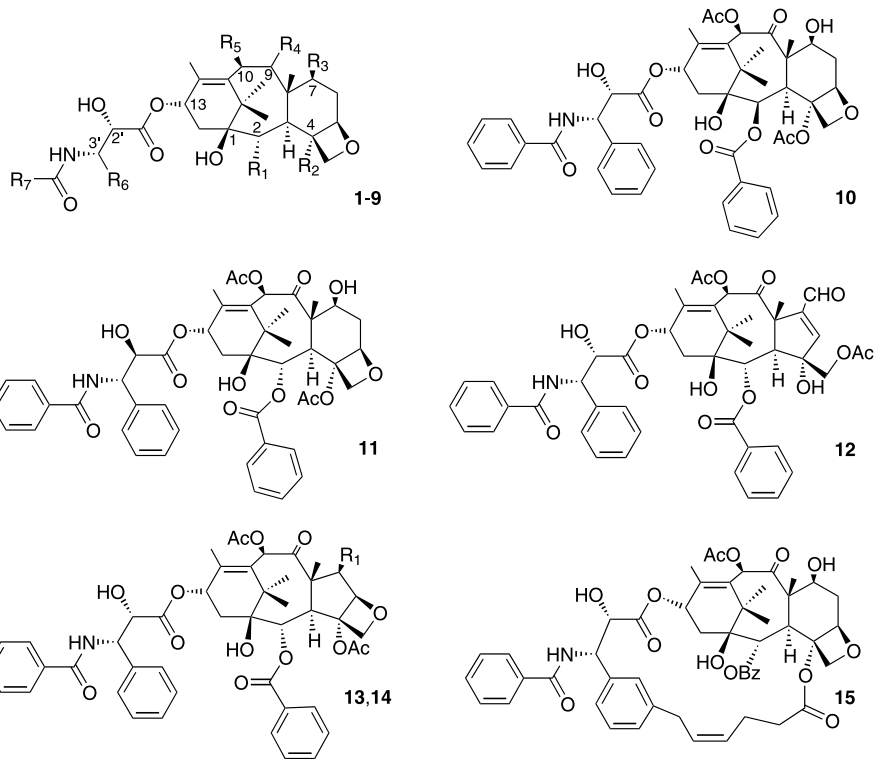

Scheme 1.

and biological activity of microtubule-stabilizing anticancer agents (MSAAs), herein, we present an atomistic pseudoreceptor model [19][1] that provides a 3D quantitative structure–activity relationship (3D QSAR) of experimentally determined and calculated binding energies of a series of taxanes. It is the first quantitative model that, starting from the experimentally determined tubulin structure, attempts to gain an insight into the specific structural features required for the ligand-receptor binding, providing further details about the influence of each pharmacophore point on the ligand-binding affinity.

2. Pseudoreceptor generation

The starting point of this work was represented by the 3D structure of the α,β-tubulin dimer (3.7 Å resolution, entry 1TUB of the Brookhaven Protein Data Bank) obtained by electron crystallography of zinc-induced tubulin sheets [20]. The experimental structure clearly showed the location of paclitaxel binding site in the β subunit but lacked the resolution to exactly define the

[1] According to the authors, the most accurate definition is "hybrid model receptor", since intermediate degrees of connectivity are present in our model. For convenience, the model has been defined as the pseudoreceptor model.

Table 1
Chemical groups of taxanes (**1**–**14**)

Comp.	R_1	R_2	R_3	R_4	R_5	R_6	R_7
1	PhCOO	AcO	OH	=O	AcO	Ph	Ph
2	H	AcO	OH	=O	AcO	Ph	Ph
3	*p*-CF_3PhCOO	AcO	OH	=O	AcO	Ph	Ph
4	PhCOO	OH	OH	=O	AcO	Ph	Ph
5	PhCOO	AcO	NH_2CH_2COO	=O	NH_2CH_2COO	Ph	*t*BuO
6	PhCOO	AcO	OH	OH	AcO	Ph	Ph
7	PhCOO	AcO	OH	=O	H	Ph	Ph
8	PhCOO	AcO	OH	=O	AcO	C_6H_{11}	Ph
9	PhCOO	AcO	OH	=O	OH	Ph	*t*BuO
13	OH						
14	AcO						

Table 2
Biological properties of taxanes (**1**–**15**) used in this study

Comp.	Activity data [a]				
	K_{exp}	K_{calc}	ΔG_{exp}	ΔG_{calc}	$\Delta\Delta G$
1	1.5×10^{-5}	7.8×10^{-6}	−6.464	−6.844	−0.380
2	4.5×10^{-3}	3.1×10^{-3}	−3.145	−3.357	−0.212
3	9.0×10^{-5}	5.1×10^{-5}	−5.421	−5.750	−0.329
4	3.0×10^{-3}	2.0×10^{-3}	−3.381	−3.608	−0.227
5	1.8×10^{-5}	2.1×10^{-5}	−6.358	−6.274	0.084
6	1.1×10^{-5}	2.3×10^{-5}	−6.635	−6.228	0.407
7	7.6×10^{-6}	3.8×10^{-6}	−6.856	−7.270	−0.414
8 [b]	4.4×10^{-6}	6.6×10^{-6}	−7.184	−6.938	0.246
9	7.1×10^{-6}	2.8×10^{-5}	−6.900	−6.103	0.797
10	4.5×10^{-3}	6.1×10^{-3}	−3.145	−2.964	0.181
11 [b]	6.0×10^{-5}	1.3×10^{-4}	−5.657	−5.227	0.430
12 [b]	3.4×10^{-3}	1.1×10^{-2}	−3.300	−2.637	0.663
13	1.2×10^{-4}	9.7×10^{-5}	−5.232	−5.376	−0.144
14	7.1×10^{-4}	7.4×10^{-4}	−4.220	−4.198	0.022
15 [b]	4.5×10^{-4}	3.4×10^{-5}	−4.480	−5.995	−1.515

[a] K_{exp}, experimental value (M); K_{calc}, calculated value (M); ΔG_{exp}, experimental value (kcal/mol); ΔG_{calc}, calculated value (kcal/mol); $\Delta\Delta G$, difference between ΔG_{exp} and ΔG_{calc}.
[b] Compounds belonging to the test set. All the remaining compounds constitute the training set.

whole ligand conformation. As a consequence, the same authors replaced paclitaxel with the X-ray structure of docetaxel [21] whose orientation in the binding site was based on the observed density for the taxane ring and one of the side-chain of paclitaxel.

From the coordinates of the tubulin-docetaxel complex, a 15-Å shell of amino acids around the ligand was selected. This subset was then pruned mainly according to site-directed mutagenesis experiments [22,23] and photoaffinity labeling studies [24–28]. The resulting 27 amino acid minireceptor (see Sections 4 and 4.2) was refined by adding hydrogen atoms and performing a conformational search on their hydroxy groups to find their proper orientation for interacting by hydrogen bonds with docetaxel. In this step, both the amino acid residues and ligand structure were kept fixed.

Next, a training set of 11 taxanes was chosen for the generation of the pseudoreceptor-inhibitors assembly. Compounds were aligned onto the conformation of docetaxel and allowed to relax within the receptor environment. Moreover, due to the fact that the tubulin structure was at low resolution, combined with the aim of removing internal strains, a preliminary optimization of the tubulin-inhibitors assembly was performed using the minimum number of ligands requested by the program [29]. In detail, three of the most active taxanes (namely compounds **1**, **7**, and **9**) were chosen as a subset to apply the ligand equilibration protocol. After this preliminary step, the pseudoreceptor with embedded training set ligands was optimized using the same equilibration protocol in order to achieve optimum interaction pattern between the ligands and the residues. The final pseudoreceptor model was characterized by a correlation coefficient (R) of 0.97 and a root mean square deviation (rmsd) of 0.35 kcal/mol (Fig. 1). Last, in the validation step, four test ligands were introduced into the pseudoreceptor and minimized keeping the pseudoreceptor fixed (rmsd for the predicted binding energies of 0.86 kcal/mol).

Superposition of the pseudoreceptor model and the corresponding experimentally determined residues showed no substantial differences, being 0.7 Å the rmsd calculated on backbone atoms.

The final conformation of **1** as derived from the pseudoreceptor modeling approach was consistent with the recently proposed T-shaped structure [30–32]. Measurement of distances and torsion angles was in good agreement with those proposed for the T-shaped or butterfly conformation of **1** instead of those proposed for the hydrophobically collapsed ones (Table 3) [33–35]. In fact, in the modeled conformation of paclitaxel, there was no hydrophobic collapse between the phenyl ring at the C3′ position and the C2 benzoyl moiety, mainly due to the presence of His229 interposed between the side-chains at C2 and C3′, thus preventing their mutual interactions. Moreover, the location of His229 was enforced by a hydrogen bond with the NH group at the C3′ position. Finally, compounds forced to hydrophobically collapse by tethering the C3′ and C2 phenyl rings, resulted to be inactive [36], supporting the hypothesis that T-shaped paclitaxel is most likely to be the biological active conformation.

3. Results and discussion

Table 2 shows a good agreement between the experimental and estimated or predicted binding values (expressed as K_i and ΔG) for the training and test set ligands, respectively.

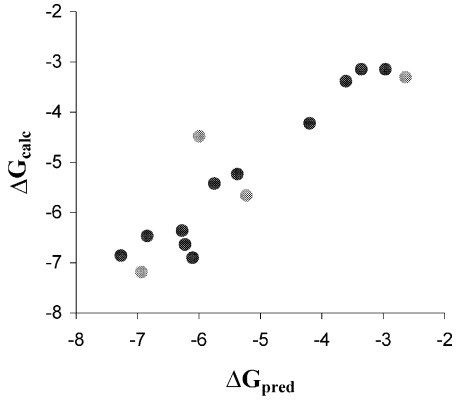

Fig. 1. Correlation line of experimentally determined ΔG_{exp} (kcal/mol) and calculated free energy ΔG_{calc} (kcal/mol) of binding for the training (black) and test set (gray).

Table 3
Comparison of the final conformation of **1** with those proposed in the literature

Paclitaxel conformations	d_1 [a]	d_2 [a]	Φ_1 [a] (°)	Φ_2 [a] (°)
Non-polar	4.7	9.8	42	−85
Polar	5.7	11.6	28	−52
T-Taxol	9.4	10.0	80	−58
1	8.2	9.9	70	−83

[a] Φ_1, Φ_2, R_1, and R_2 are calculated according to Ref. [30]. Φ_1 and Φ_2 are the improper torsion angles O–C2–C3′–N(Bz) and O–C2–C3′–C(Ph) of paclitaxel, respectively. d_1 and d_2 are the distances (in Å) from the centroid of the C2 benzoyl phenyl ring and the centroid of the C3′–N(Bz) phenyl ring, and the centroid of the C2 benzoyl phenyl ring and the C3′ phenyl ring, respectively.

Fig. 2 depicts the interaction pathway between paclitaxel (compound **1**, taken as a representative example of all taxanes considered in this study). In detail, the model is mainly represented by several hydrophobic pockets also establishing hydrogen bonds with taxanes. On the other hand, the macrocycle core structure of **1** retains the optimal conformation to bring its side-chains on the proper orientation to interact with the protein. Residues Leu217, Leu219, Asp226, and His229 are located close to the C2 benzoyl group, while Lys19, Val23, and Asp26 are found around the C3′ benzamide moiety. Finally, Thr276, Ser277, and Arg278 surround the C7 position of **1**. It is very important to note that this disposition of residues around the ligand is in perfect agreement with photoaffinity labeling studies [24–28].

In addition, tubulin–ligands interactions found in the model are all consistent with structure–activity relationship data collected from the literature. In fact (i) as far as the ''northern'' part of **1** (C10, C9, and C7 positions), only the C7 hydroxy group is engaged in an electrostatic interaction with the side-chain of Thr276. In addition to the C7 hydroxy group of **1**, different hydrogen bond donor functions (i.e., the aminoacetyl moiety of compound **5**) are allowed to interact with the protein. This finding well accounts for the about two orders of magnitude decreased activity found for compound **14** bearing an acetyl group instead of a C7 hydrogen bond donor function ($K_{exp} = 7.1 \times 10^{-4}$ M, $K_{calc} = 7.4 \times 10^{-4}$ M). Compound **13** is characterized by a contracted five-membered C ring. Consequently, the C7 hydroxy group is moved away from Thr276 and the corresponding hydrogen bond results to be more stressed and less effective. In fact, due to the different location of the C7–OH, although the proper hydrogen bond distance between this group and the Thr276 side-chain was retained, the proper angle required to establish such a kind of interaction was lost. K_{calc} of **13** has been estimated by the model to be 9.7×10^{-5} M, in agreement with the experimentally determined values of 1.2×10^{-4} M. Even if 7-deoxy analogues are reported to possess activity similar to paclitaxel [37–40], it is also known that only polar groups are tolerated without modifying ligand activity [41,42]. Accordingly, replacement of C7–OH by a hydrophobic group produces an unfavorable hydrophobic–polar interaction with the side-chain of Thr276 with a consequent deep decrease in activity. Moreover, according to mutagenesis studies, the substitution of Thr276 with Ile results in the location of the C7–OH into a less favorable hydrophobic context [22]. All these considerations led to the suggestion that the substituent at the C7 position is located within a hydrophilic area, also including the hydroxy side-chain of Thr276, able to form a hydrogen bond with the C7

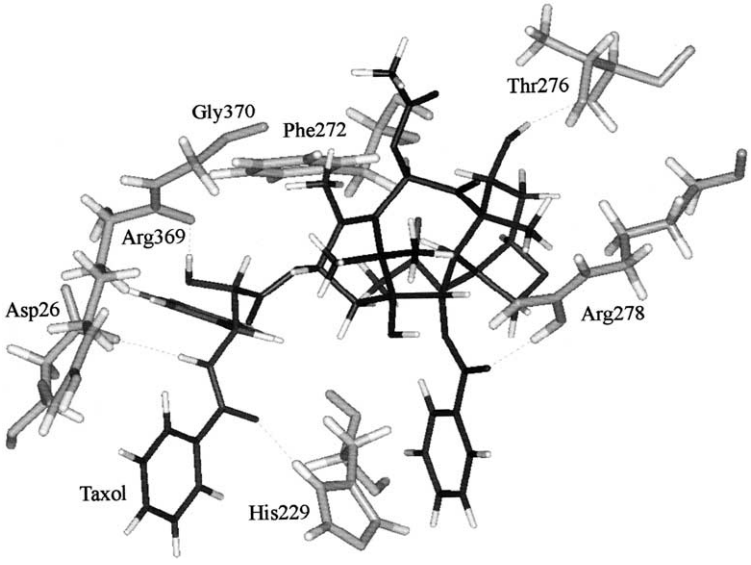

Fig. 2. Paditaxel, taken as a representative of all taxanes used in this study, fitted into the pseudoreceptor model. For sake of clarity, only the most important ligand–protein interactions have been evidenced.

hydroxy function of **1**, as found in the pseudoreceptor model.

(ii) It has been reported in the literature that C9 and C10 positions can be manipulated without modifying the activity [37–39,43–48]. In the pseudoreceptor model, the C10 acetyl group of **1** is projected away from the binding pocket without any profitable interaction with amino acid residues. On the other hand, the presence of a hydrogen bond donor function allows compound **5**, characterized by a C10 aminoacetyl moiety, and compound **9**, characterized by a C10 hydroxy group, to form a hydrogen bond with Gly370.

(iii) Although reduction of the carbonyl group at the C9 position is reported to slightly improve activity [49,50], no interaction between this moiety and the protein has been found in the pseudoreceptor model. On the other hand, compound **6** is correctly estimated to be more active than paclitaxel due to the fact that in addition to the usual C7–OH/Thr276 interaction, an intramolecular hydrogen bond involving the C9 and C7 hydroxy groups was found that stabilizes the conformation of this ligand inside the protein ($K_{exp} = 1.1 \times 10^{-5}$ M, $K_{calc} = 2.3 \times 10^{-5}$ M).

(iv) Regarding the oxetane moiety, the importance of the four-membered ring has been discussed for a long time, leading to the hypothesis that this group constitutes a lock on the taxoid skeleton and represents a hydrogen bond acceptor feature [51–56], but, at the same time, it is not absolutely required. The oxetane ring is not involved in any interaction with the binding site of the pseudoreceptor model, although located near the same cluster of polar residues to which Thr276 belongs. One of the test set compounds (**12**) with an opened D-ring is predicted to be about three orders of magnitude less active than paclitaxel which is in good agreement with the experimental data ($K_{exp} = 3.4 \times 10^{-3}$ M, $K_{calc} = 1.1 \times 10^{-2}$ M). Although it lacks the C7 hydroxy group and consequently the hydrogen bond with Thr276, the opening of the oxetane ring causes a different location for the C4 acetyl moiety and the unfavorable location of the polar C4–OH in a hydrophobic cleft. This fact supports the hypothesis of the rigidification role of oxetane ring.

(v) C4 and C2 substituents play essential roles in the tubulin–ligand interaction. In particular, the C4 acetyl group lies in a deep hydrophobic cleft of the pseudoreceptor model which is in agreement with what reported in the literature [57]. When the acetyl group is substituted by a polar hydroxy side-chain (as in compound **4**) so that the corresponding hydrophobic contact with tubulin is lost, a decrease of about two orders of magnitude in activity is found ($K_{exp} = 3.0 \times 10^{-3}$ M, $K_{calc} = 2.0 \times 10^{-3}$ M). The hydrophobic character of this pocket is satisfied by compound **15**, possessing a long alkyl chain connecting the C4 acetyl group to the meta-position of the C3′ phenyl ring. Despite the structural rigidification leading to the loss of the two usual hydrogen bonds between both C3′–NH and C7–OH with the protein, the hydrophobic interaction between the long alkyl chain and the model counterbalances for the lacking of electrostatic interactions in such a way that compound **15** is overestimated of about one order of magnitude.

(vi) The carbonyl group of the C2 benzoyl moiety is engaged in a hydrogen bond with Arg278. Removal of the benzoyl group (as in compound **2**) or the impossibility to contact Arg278 (as in compound **10**) leads to a loss of activity, estimated to be more than two orders of magnitude lower than the corresponding parent compound **1** which is in agreement with the experimental data ($K_{exp} = 4.5 \times 10^{-3}$ M, $K_{calc} = 3.1 \times 10^{-3}$ M for compound **2**; $K_{exp} = 4.5 \times 10^{-3}$ M, $K_{calc} = 6.1 \times 10^{-3}$ M for compound **10**). *para*-Substitution of compound **3** causes a slight reduction of activity with respect to **1** [58], due to the steric requirements of the pseudoreceptor pocket defined by His229, Asp226, and Lys19, accommodating the C2 benzoyl moiety. On the contrary, the pseudoreceptor model shows one of the meta-positions free to accommodate a substitution moiety, in agreement with literature data proving that *meta*-substitution enhances activity [67].

(vii) The C1 hydroxy group seems to play only a small role on the overall bioactivity of paclitaxel [59]. Accordingly, this group does not interact with the protein model but contributes to the ligand stability through an electrostatic interaction with the carbonyl group of the C2 benzoyl moiety.

(viii) The C13 side-chain has been considered essential for activity of taxanes. However, biological evaluation of baccatin III analogues differing from **1** for the absence of this moiety [37,60] leads to the conclusion that the C13 side-chain mainly provides a specific anchor function for paclitaxel binding [61].

Structural features of the C13 side-chain are able to provide profitable interactions with the protein. Accordingly, our model shows the carbonyl group of Arg369 as a hydrogen bond acceptor for interactions with the C2′ hydroxy group, whose essential role has been demonstrated [55,56] together with its hydrogen bond donor property [62]. Compound **11** is predicted to be less active than **1** ($K_{exp} = 6.0 \times 10^{-5}$ M, $K_{calc} = 1.3 \times 10^{-4}$ M) due to the inverted stereochemistry at both the C2′ and C3′ positions. Chiral changes cause the C2′ hydroxy group being pointed away from Arg369 and unable to form any electrostatic interaction with it. In addition to the C2′ hydroxy group, the amide moiety at the C3′ position is engaged in interactions with tubulin, both the NH and the carbonyl group being involved in hydrogen bonds with Asp26 and His229, respectively. In the model, these interactions are responsible for the anchor function of C13 inside the binding pocket, also contributing to the T-shaped conformation of paclitaxel.

The C3′ phenyl ring of **1** is located in a large pocket of the model also able to accommodate the C3′ cyclohexyl group of compound **8**, well accounting for its higher activity with respect to **1** ($K_{exp} = 4.4 \times 10^{-6}$ M, $K_{calc} = 6.6 \times 10^{-6}$ M). The pocket where the C3′ moiety lies includes Phe272 and Ser374. As demonstrated in literature, a Phe272Val mutation causes the missing of the hydrophobic interaction with the C3′ moiety, while mutation of Ser374 causes a structural reorganization of the above-described amino acid subset including a conformational rearrangement of the Phe272, affording paclitaxel resistance [22].

3.1. Comparison with previously proposed models

Many attempts have been reported in the literature to develop a pharmacophore model for taxanes (i.e., CoMFA studies) [63–65] or for paclitaxel mimics [66]. All these approaches are affected by several limitations due to the lack of protein environment and for using a rigid conformational template to model the paclitaxel analogues. A first effort to deal with this problem is represented by the minireceptor approach applied by Snyder et al. [67] to the creation of a binding site for a training set of taxanes and epothilones. However, the depicted protein environment is characterized by significant structural differences with respect to the electron crystallography structure of α,β-tubulin at the level of both amino acid types and their location around the ligands. Moreover, the paclitaxel conformation resulting from pseudoreceptor modeling approach in Snyder's paper is the typical hydrophobically collapsed one which is in contrast with the recent studies by the same group supporting the T-shaped paclitaxel as the bioactive conformation [30–32].

All these differences between the constructed [67] and our experimentally derived pseudoreceptor model lead to the suggestion that the latter one is the more reliable in representing the paclitaxel–tubulin complex.

Based on the availability of the electron crystallography structure of tubulin, many studies have been performed, most of them being directed toward the identification of paclitaxel conformation to be subsequently fitted in the unmodified or refined tubulin binding site [35,68–70]. An interesting model for the binding of **1** to β-tubulin has been recently proposed by Snyder et al. [30]. The major difference with the model described in this paper is represented by the role of the oxetane ring. In our model, the four-membered ring only functions as a lock for paclitaxel macrocycle, while in the Snyder's model it is engaged in an electrostatic interaction with the protein. In addition, different from our pseudoreceptor model, no quantitative considerations can be made by means of the Snyder's model.

Indeed, the pseudoreceptor model discussed in the present paper takes into account two important aspects of modeling studies: (1) generation of a pharmacophore model for taxanes and fitting of this pharmacophore into a binding site derived from the experimental coordinates of tubulin; (2) elaboration of a theoretical model correlating at a quantitative level the structural properties of ligands with their biological data (3D QSAR model). Both the fitting and the 3D QSAR steps are developed simultaneously avoiding the limitation suffered by the other models in considering in separate steps the 3D properties of the ligands or refinement of the protein. As an example, although the hydrophobically collapsed conformation of **1** has been used as the input, PrGen protocol is not bound to this structure, showing a T-shaped conformer as the putative biological conformation of paclitaxel.

4. Methods

4.1. Ligand construction

Compounds belonging to the family of taxanes used to build the training set have been collected from the literature [71,72] on the basis of structural similarity in the widest range of biological activity, under the assumption that all substances are acting through the paclitaxel–tubulin binding site. They are characterized by affinity values expressed as IC_{50} or EC_{50}, in turn expressed as rough K_i spanning over ~ 2.5 orders of magnitude, the minimum value of 7.1 μM being associated with docetaxel and the maximum value of 3000 μM being associated with compound **4**.

The conformation of docetaxel embedded in the tubulin structure has been considered as the bioactive one and used as a template to drive modeling of the conformation of all the remaining taxanes belonging to both the training and test set.

After calculation of MNDO atomic partial charges by means of MOPAC 6 [73], molecules were minimized using YETI force field [74] (both implemented in PrGen software) to obtain strain-free conformers and calculate their energy values [29]. In addition, the relaxed conformations have been used to calculate solvation energies ($\Delta G_{solvation,ligand}$) based on the method of Still et al. [75], as well as the loss of entropy upon receptor binding ($T\,\Delta S_{binding}$) based on the method of Searle and Williams [76].

Taking into account the Gibbs–Helmhotz equation, the conversion of experimental K_i to free energies of binding was calculated as follows:

$$\Delta G^0 = RT \ln K_i$$

4.2. Pseudoreceptor modeling

The training set was subsequently used to calibrate the 27 amino acid pseudoreceptor model (namely Lys19, Val23, Asp26, Leu217, Leu219, Asp226, His229, Leu230, Ser232, Ala233, Ser236, Thr240, Phe244, Phe272, Pro274, Leu275, Thr276, Ser277, Arg278, Arg320, Ile358, Pro360, Arg369, Gly370, Leu371, Ser374, and Thr376). The ligand equilibration protocol allows to obtain a high correlation between observed and calculated free energies of binding for the ligands of the training set. In the first step, the receptor is subjected to an energy minimization of all residues, keeping position, orientation, and conformation of the training set ligands unaltered. A additional term, referred to as correlation coupling, is introduced to couple the actual rmsd of ΔG_{exp} and ΔG_{cal} to the force field energy of the system. By a straightforward minimization of this term during the correlation-coupled minimization of the receptor, a high correlation can be enforced.

In a second step, the ligands are allowed to relax within the receptor to remove all the strains probably imposed by the previous step. Ligands are minimized while receptor residues are kept fixed, usually leading to a less correlated model. Correlation-coupled receptor minimization and unconstrained ligand relaxation are repeated until a high correlated pseudoreceptor model is obtained. In this study, a coupling constant of 1.0 and a maximal allowed rms of 0.197 kcal/mol for the predicted versus experimental ΔG of all correlation-coupled minimization procedures were used.

Free energies of ligand binding ΔG^0_{pred} are obtained by means of a linear regression (slope a and intercept b) between ΔG^0_{exp} and $E_{binding}$ calculated for the training set ligands:

$$\Delta G^0_{pred} = |a| E_{binding} + b$$

where $E_{binding}$ is calculated using the following approximation proposed by Blaney et al. [77].

$$E_{binding} \cong E_{ligand\text{-}receptor} - T\,\Delta S_{binding} - \Delta G_{solvation,ligand} + \Delta E_{internal,ligand}$$

In a validation step, a test set of ligands is used to examine the ability of the receptor model in predicting free energies of binding. The test set is relaxed within the fixed binding pocket applying the same protocol used for the training set ligands. The linear regression obtained for the training set is used to predict free energies of binding for the test set compounds.

5. Conclusions

The antimitotic agents, paclitaxel and docetaxel, have been demonstrated to have efficacy in the treatment of breast, ovarian, and lung cancers. Although they have importance in anticancer chemotherapy, they possess some disadvantages represented by resistant cancers or toxic side effects. For these reasons, design of new taxanes with improved biological activity is still an important research subject.

A quantitative 3D model for the binding site of taxanes has been generated for the first time, starting from the experimental coordinates of the paclitaxel–tubulin complex. The pseudoreceptor obtained by means of PrGen software provided a good correlation between the experimental and calculated binding energies for a training set of taxanes. The model identified the pharmacophore features of the ligands and the relative counterparts on the tubulin binding site, mainly interacting by hydrogen bonds and hydrophobic contacts. Hydrogen bonds involved the C2 benzoyl, C7 hydroxy, C2′ hydroxy, and C3′ amido groups of ligands. Moreover, a hydrophobic pocket surrounding the C3′ phenyl ring and C4 acetyl moiety was found, while the C2 benzoyl and C3′ benzamide functions lie in two different subsites of the pseudoreceptor. The equilibration protocol allowed the model to estimate or predict binding affinities for training and test set ligands, respectively, which is in good agreement with the experimental data. Moreover, analysis of the paclitaxel conformers into the pseudoreceptor model led to the conclusion that the T-shaped is the conformation adopted by taxanes to interact with tubulin. Considering that the search for taxanes with improved activity with respect to **1** is always a crucial point in anticancer therapy, this model could be useful for predicting binding affinity of new compounds and for a rational design approach leading to new taxanes with improved affinity toward tubulin.

Moreover, it can be anticipated that the present paclitaxel–tubulin model is ongoing to be improved by incorporating more paclitaxel mimics in the training set in order to develop a common pharmacophore model for all the compounds proved to be microtubule-stabilizing agents.

Acknowledgements

Support from the Research Training Network (HPRN-CT-2000-00018) "Design and Synthesis of Novel Paclitaxel (Taxol) Mimics Using a Common Pharmacophore Model for Microtubule-stabilising Anticancer Agents (MSAAs)" is gratefully acknowledged. One of us (M.B.) thanks the Merck Research Laboratories for the 2002 Academic Development Program (ADP) Chemistry Award. We are all indebted to Dr. J.P. Snyder for suggestions and fruitful discussion. The authors wish to thank the "Centro Universi-

tario per l'Informatica e la Telematica'' of the University of Siena.

References

[1] A.K. Singla, A. Garg, D. Aggarwal, Paclitaxel and its formulations, Int. J. Pharm. 235 (2002) 179–192.

[2] W.J. Slichenmyer, D.D. Von Hoff, Taxol: a new and effective anti-cancer drug, Anticancer Drugs 2 (1991) 519–530.

[3] L.R. Wiseman, C.M. Spencer, Paclitaxel: an update of its use in the treatment of metastatic breast cancer and ovarian and other gynaecological cancers, Drugs Aging 12 (1998) 305–334.

[4] S.B. Horwitz, Taxol (paclitaxel): mechanisms of action, Ann. Oncol. 5 (Suppl. 6) (1994) S3–S6.

[5] W.B. Derry, L. Wilson, M.A. Jordan, Substoichiometric binding of Taxol suppresses microtubule dynamics, Biochemistry 34 (1995) 2203–2211.

[6] E. Hamel, Antimitotic natural products and their interactions with tubulin, Med. Res. Rev. 16 (1996) 207–231.

[7] P.B. Schiff, J. Fant, S.B. Horwitz, Promotion of microtubule assembly in vitro by Taxol, Nature 277 (1979) 665–667.

[8] L. Wilson, M.A. Jordan, Microtubule dynamics: taking aim at a moving target, Chem. Biol. 2 (1995) 569–573.

[9] P.B. Schiff, S.B. Horwitz, Taxol stabilizes microtubules in mouse fibroblast cells, Proc. Natl. Acad. Sci. USA 77 (1980) 1561–1565.

[10] K.H. Altmann, M. Wartmann, T. O'Reilly, Epothilones and related structures: a new class of microtubule inhibitors with potent in vivo antitumor activity, Biochim. Biophys. Acta 1470 (2000) M79–M91.

[11] R. Balachandran, E. ter Haar, M.J. Welsh, S.G. Grant, B.W. Day, The potent microtubule-stabilizing agent (+)-discodermolide induces apoptosis in human breast carcinoma cells: preliminary comparisons to paclitaxel, Anticancer Drugs 9 (1998) 67–76.

[12] M. Roberge, B. Cinel, H.J. Anderson, L. Lim, X. Jiang, L. Xu, C.M. Bigg, M.T. Kelly, R.J. Andersen, Cell-based screen for antimitotic agents and identification of analogues of rhizoxin, eleutherobin, and paclitaxel in natural extracts, Cancer Res. 60 (2000) 5052–5058.

[13] E. Hamel, D.L. Sackett, D. Vourloumis, K.C. Nicolaou, The coral-derived natural products eleutherobin and sarcodictyins A and B: effects on the assembly of purified tubulin with and without microtubule-associated proteins and binding at the polymer taxoid site, Biochemistry 38 (1999) 5490–5498.

[14] S.L. Mooberry, G. Tien, A.H. Hernandez, A. Plubrukarn, B.S. Davidson, Laulimalide and isolaulimalide, new paclitaxel-like microtubule-stabilizing agents, Cancer Res. 59 (1999) 653–660.

[15] M. Rosner, H.G. Capraro, A.E. Jacobson, L. Atwell, A. Brossi, M.A. Iorio, T.H. Williams, R.H. Sik, C.F. Chignell, Biological effects of modified colchicines: improved preparation of 2-dimethylcolchicine, 3-dimethylcolchicine, and (+)-colchicine and reassignment of the position of the double bond in dehydro-7-deacetamidocolchicines, J. Med. Chem. 24 (1981) 257–261.

[16] R.L. Noble, C.T. Beer, J.H. Cutts, Role of chance observation in chemotherapy, Ann. NY Acad. Sci. 76 (1958) 882–894.

[17] L. Wilson, M.A. Jordan, Microtubule dynamics: taking aim at a moving target, Chem. Biol. 2 (1995) 569–573.

[18] K.H. Altmann, Microtubule-stabilizing agents: a growing class of important anticancer drugs, Curr. Opin. Chem. Biol. 5 (2001) 424–431.

[19] A. Vedani, P. Zbinden, J.P. Snyder, P.A. Greenidge, Pseudoreceptor modeling: the construction of three-dimensional receptor surrogates, J. Am. Chem. Soc. 117 (1995) 4987–4994.

[20] E. Nogales, S.G. Wolf, K.H. Downing, Structure of the a β-tubulin dimer by electron crystallography, Nature 391 (1998) 199–203.

[21] F. Gueritte-Voegelein, D. Guenard, L. Mangatal, P. Potier, J. Guilhem, M. Cesario, Structure of a synthetic Taxol precursor: *N*-*tert*-butoxycarbonyl-10-deacetyl-*N*-debenzoyltaxol, Acta Crystallogr. C 46 (1990) 781–784.

[22] P. Giannakakou, D.L. Sackett, Y.K. Kang, Z. Shan, J.T.M. Buters, T. Fojo, M.S. Poruchynsky, Paclitaxel-resistant human ovarian cancer cells have mutant β-tubulins that exhibit impaired paclitaxel-driven polymerization, J. Biol. Chem. 272 (1997) 17118–17125.

[23] M.L. Gonzalez-Garay, L. Chang, K. Blade, D.R. Menick, F. Cabral, A β-tubulin leucine cluster involved in microtubule assembly and paclitaxel resistance, J. Biol. Chem. 274 (1999) 23875–23882.

[24] S. Rao, G.A. Orr, A.G. Chaudhary, D.G.I. Kingston, S.B. Horwitz, Characterization of the Taxol binding site on the microtubule: 2-(*m*-azidobenzoyl)taxol photolabels a peptide (amino acids 217–231) of β-tubulin, J. Biol. Chem. 270 (1995) 20235–20238.

[25] D. Mastropaolo, A. Camerman, Y. Luo, G.D. Brayer, Crystal and molecular structure of paclitaxel (Taxol), Proc. Natl. Acad. Sci. USA 92 (1995) 6920–6924.

[26] S. Rao, S.B. Horwitz, I. Ringel, Direct photoaffinity labeling of tubulin with Taxol, J. Natl. Cancer Inst. 84 (1992) 785–788.

[27] S. Rao, N.E. Krauss, J.M. Heerding, C.S. Swindell, I. Ringel, G.A. Orr, S.B. Horwitz, 3′-(*p*-Azidobenzamido)taxol photolabels the N-terminal 31 amino acids of β-tubulin, J. Biol. Chem. 269 (1994) 3132–3134.

[28] D. Dasagupta, H. Park, G.C.B. Harriman, G.I. Georg, R. Himes, Synthesis of a photoaffinity Taxol analog and its use in labeling tubulin, J. Med. Chem. 37 (1994) 2976–2980.

[29] P. Zbinden, M. Dobler, G. Folkers, A. Vedani, PrGen: pseudoreceptor modeling using receptor-mediated ligand alignment and pharmacophore equilibration, Quant. Struct.-Act. Relat. 17 (1998) 122–130.

[30] J.P. Snyder, J.H. Nettles, B. Cornett, K.H. Downing, E. Nogales, The binding conformation of Taxol in β-tubulin: a model based on electron crystallographic density, Proc. Natl. Acad. Sci. USA 98 (2001) 5312–5316.

[31] M. Milanesio, P. Ugliengo, D. Viterbo, G. Appendino, Ab initio conformational study of the phenylisoserine side chain of paclitaxel, J. Med. Chem. 42 (1999) 291–299.

[32] J.P. Snyder, N. Nevins, D.O. Cicero, J.J. Jansen, The conformations of Taxol in chloroform, J. Am. Chem. Soc. 122 (2000) 724–725.

[33] D.G. Vander Velde, G.I. Georg, G.L. Grunewald, C.W. Gunn, L.A. Mitscher, ''Hydrophobic collapse'' of Taxol and Taxotere solution conformations in mixtures of water and organic solvent, J. Am. Chem. Soc. 115 (1993) 11650–11651.

[34] I. Ojima, S.D. Kuduk, S. Chakravarty, M. Ourevitch, J.P. Begue, A novel approach to the study of solution structures and dynamic behavior of paclitaxel and docetaxel using fluorine-containing analogs as probes, J. Am. Chem. Soc. 119 (1997) 5519–5527.

[35] Y. Li, B. Poliks, L. Cegelski, M. Poliks, Z. Gryczynski, G. Piszczek, P.G. Jagtap, D.R. Studelska, D.G.I. Kingston, J. Schaefer, S. Bane, Conformation of microtubule-bound paclitaxel determined by fluorescence spectroscopy and REDOR NMR, Biochemistry 39 (2000) 281–291.

[36] T.C. Boge, Z.J. Wu, R.H. Himes, D.G. Vander Velde, G.I. Georg, Conformationally restricted paclitaxel analogues: macrocyclic mimics of the ''hydrophobic collapse'' conformation, Bioorg. Med. Chem. Lett. 9 (1999) 3047–3052.

[37] H. Poujol, A. Al Mourabit, A. Ahond, C. Poupat, P. Potier, Taxoïdes: 7-déshydroxy-10-acétyldocétaxel et nouveaux analogues préparés à partir des alcaloïdes de l'if, Tetrahedron 53 (1997) 12575–12594.
[38] R.N. Saicic, R. Matovic, An efficient semisynthesis of 7-deoxypaclitaxel from taxine, J. Chem. Soc., Perkin Trans. 1 (2000) 59–66.
[39] P.H.G. Wiegerinck, L. Fluks, J.B. Hammink, S.J.E. Mulders, F.M.H. de Groot, H.L.M. van Rozendaal, Semisynthesis of some 7-deoxypaclitaxel analogs from taxine B, J. Org. Chem. 61 (1996) 7092–7100.
[40] H. Poujol, A. Al Mourabit, A. Ahond, A. Chiaroni, C. Poupat, C. Riche, P. Potier, Taxoïdes: nouveaux analogues du 7-déshydroxydocétaxel préparés à partir des Alcaloïdes de l'if, Tetrahedron 53 (1997) 5169–5184.
[41] D. Guenard, S. Thoret, J. Dubois, M.T. Adeline, Q. Wang, F. Gueritte, Effects of the hydrophobicity of taxoids on their interaction with tubulin, Bioorg. Med. Chem. 8 (2000) 145–156.
[42] S. Lin, I. Ojima, Recent strategies in the development of taxane anticancer drugs, Exp. Opin. Ther. Patents 10 (2000) 869–889.
[43] A.G. Chaudhary, D.G.I. Kingston, Synthesis of 10-deacetoxytaxol and 10-deoxytaxotere, Tetrahedron Lett. 34 (1993) 4921–4924.
[44] D.G.I. Kingston, in: G.I. Georg, T.T. Chen, I. Ojima, D.M. Vyas (Eds.), Taxane Anticancer Agents, ACS Symposium Series, Vol. 583, American Chemical Society, Washington, DC, 1995, p. 203.
[45] S.H. Chen, S. Huang, J. Kant, C. Fairchild, J.M. Wei, V. Farina, Synthesis of 7-deoxy- and 7,10-dideoxytaxol via radical intermediates, J. Org. Chem. 58 (1993) 5028–5029.
[46] G.I. Georg, Z.S. Cheruvallath, Samarium diiodide-mediated deoxygenation of Taxol: a one-step synthesis of 10-deacetoxytaxol, J. Org. Chem. 59 (1994) 4015–4018.
[47] R.A. Holton, C. Somoza, K.B. Chai, A simple synthesis of 10-deacetoxytaxol derivatives, Tetrahedron Lett. 35 (1994) 1665–1668.
[48] J.P. Pulicani, H. Bouchard, J.D. Bourzart, A. Commerçon, Preparation of 7-modified docetaxel analogs using electrochemistry, Tetrahedron Lett. 35 (1994) 9709–9712.
[49] L.L. Klein, Synthesis of 9-dihydrotaxol: a novel bioactive taxane, Tetrahedron Lett. 34 (1993) 2047–2050.
[50] L.L. Klein, L. Li, C.J. Maring, C.M. Yeung, S.A. Thomas, D.J. Grampovnik, J.J. Plattner, Antitumor activity of 9(*R*)-dihydrotaxane analogs, J. Med. Chem. 38 (1995) 1482–1492.
[51] F. Gueritte, General and recent aspects of the chemistry and structure–activity relationships of taxoids, Curr. Pharm. Des. 7 (2001) 1229–1249.
[52] M. Gurrath, G. Muller, H.D. Holtje, Perspective in Drug Discovery Today, vol. 12–14, 1998, pp. 155–157.
[53] M. Wang, B. Cornett, J. Nettles, D.C. Liotta, J.P. Snyder, The oxetane ring in Taxol, J. Org. Chem. 65 (2000) 1059–1068.
[54] L. Barboni, A. Datta, D. Dutta, G.I. Georg, D.G. Vander Velde, R.H. Himes, M. Wang, J.P. Snyder, Novel D-seco paclitaxel analogues: synthesis, biological evaluation and model testing, J. Org. Chem. 66 (2001) 3321–3329.
[55] F. Gueritte-Voegelein, D. Guenard, F. Lavell, M.T. LeGoff, L. Mangatal, P. Potier, Relationships between the structure of Taxol analogs and their antimitotic activity, J. Med. Chem. 34 (1991) 992–998.
[56] C.S. Swindell, N.E. Krauss, S.B. Horwitz, I. Ringel, Biologically active Taxol analogues with deleted A-ring side chain substituents and variable C-2′ configurations, J. Med. Chem. 34 (1991) 1176–1184.
[57] S.H. Chen, J.M. Wei, B.H. Long, C.A. Fairchild, J. Carboni, W.W. Mamber, W.C. Rose, K. Johnston, A.M. Casazza, J.F. Kadow, Novel C-4 paclitaxel (Taxol®) analogs: potent antitumor agents, Bioorg. Med. Chem. Lett. 5 (1995) 2741–2746.
[58] A.G. Chaudhary, M.M. Gharpure, J.M. Rimoldi, M.D. Chordia, A.A.L. Gunatilaka, D.G.I. Kingston, S. Grover, C. Lin, E. Hamel, Unexpectedly facile hydrolysis of the 2-benzoate group of Taxol and syntheses of analogs with increased activities, J. Am. Chem. Soc. 116 (1994) 4097–4098.
[59] D.G.I. Kingston, M.D. Chordia, P.G. Jagtap, J. Liang, Y.C. Shen, B.H. Long, C.R. Fairchild, K.A. Johnston, Synthesis and biological evaluation of 1-deoxypaclitaxel analogues, J. Org. Chem. 64 (1999) 1814–1822.
[60] H. Lataste, V. Senhil, M. Wright, D. Guenard, P. Potier, Relationship between the structures of Taxol and baccatin III and their in vitro action on the disassembly of mammalian brain and Physarum amoebal microtubules, Proc. Natl. Acad. Sci. USA 81 (1984) 4090–4094.
[61] J.M. Andreu, I. Barasoain, The interaction of baccatin III with the Taxol binding site of microtubules determined by a homogeneous assay with fluorescent taxoid, Biochemistry 40 (2001) 11975–11984.
[62] H.J. Williams, G. Moyna, A.I. Scott, C.S. Swindell, L.E. Chirlian, J.M. Heerding, D.K. Williams, NMR and molecular modeling study of the conformations of Taxol 2′-acetate in chloroform and aqueous dimethyl sulfoxide solutions, J. Med. Chem. 39 (1996) 1555–1559.
[63] K.H.A. Czaplinski, G.L. Grunewald, A comparative molecular field analysis derived model of the binding of Taxol® analogues to microtubules, Bioorg. Med. Chem. Lett. 4 (1994) 2211–2216.
[64] Q. Zhu, Z. Guo, N. Huang, M. Wang, F. Chu, Comparative molecular field analysis of a series of paclitaxel analogues, J. Med. Chem. 40 (1997) 4319–4328.
[65] H. Morita, A. Gonda, L. Wei, K. Takeya, H. Itokawa, 3D QSAR analysis of taxoids from *Taxus cuspidata* var. nana by comparative molecular field approach, Bioorg. Med. Chem. Lett. 7 (1997) 2387–2392.
[66] I. Ojima, S. Chakravarty, T. Inoue, S. Lin, L. He, S.B. Horwitz, S.D. Kuduk, S.J. Danishefsky, A common pharmacophore for cytotoxic natural products that stabilize microtubules, Proc. Natl. Acad. Sci. USA 96 (1999) 4256–4261.
[67] M. Wang, X. Xia, Y. Kim, D. Hwang, J.M. Jansen, M. Botta, D.C. Liotta, J.P. Snyder, A unified and quantitative receptor model for the microtubule binding of paclitaxel and epothilone, Org. Lett. 1 (1999) 43–46.
[68] L. He, P.G. Jagtap, D.G.I. Kingston, H.J. Shen, G.A. Orr, S.B. Horwitz, A common pharmacophore for Taxol and the epothilones based on the biological activity of a taxane molecule lacking a C-13 side chain, Biochemistry 39 (2000) 3972–3978.
[69] P. Giannakakou, R. Gussio, E. Nogales, K.H. Downing, D. Zaharevitz, B. Bollbuck, G. Poy, D. Sackett, K.D. Nicolaou, T. Fojo, A common pharmacophore for epothilone and taxanes: molecular basis for drug resistance conferred by tubulin mutations in human cancer cells, Proc. Natl. Acad. Sci. USA 97 (2000) 2904–2909.
[70] L.A. Martello, M.J. LaMarche, L. He, T.J. Beauchamp, A.B. Smith, III, S.B. Horwitz, The relationship between Taxol and (+)-discodermolide: synthetic analogs and modeling studies, Chem. Biol. 8 (2001) 843–855.
[71] F. Gueritte-Voegelein, D. Guenard, F. Lavelle, M.T. Le Goff, L. Mangatal, P. Potier, Relationships between the structure of Taxol analogs and their antimitotic activity, J. Med. Chem. 34 (1991) 992–998.
[72] B.B. Metaferia, J. Hoch, T.E. Glass, S.L. Bane, S.K. Chatterjee, J.P. Snyder, A. Lakdawala, B. Cornett, D.G. Kingston, Synthesis and biological evaluation of novel macrocyclic paclitaxel analogues, Org. Lett. 3 (2001) 2461–2464.

[73] J.J.P. Stewart, MOPAC, J. Comput. Aided Mol. Des. 4 (1990) 1.
[74] A. Vedani, D.W. Huhta, A new force field for modeling metalloproteins, J. Am. Chem. Soc. 112 (1990) 4759–4767.
[75] W.C. Still, A. Tempczyk, R.C. Hawley, T. Hendrickson, Semianalytical treatment of solvation for molecular mechanics and dynamics, J. Am. Chem. Soc. 112 (1990) 6127–6129.
[76] M.S. Searle, D.H. Williams, The cost of conformational order: entropy changes in molecular associations, J. Am. Chem. Soc. 114 (1992) 10690–10697.
[77] J.M. Blaney, P.K. Weiner, A. Dearing, P.A. Kollman, E.C. Jorgensen, S.J. Oatley, J.M. Burridge, J.F. Blake, Molecular mechanics simulation of protein–ligand interactions: binding of thyroid hormone analogs to prealbumin, J. Am. Chem. Soc. 104 (1984) 6424–6434.